The Astrophysical Journal, 860:139 (5pp), 2018 June 20 https://doi.org/10.3847/1538-4357/aac6ee

Are Small Radii of Compact Stars Ruled out by GW170817/AT2017gfo?

G. F. Burgio[1], A. Drago[2], G. Pagliara[2], H.-J. Schulze[1], and J.-B. Wei[1]
[1] INFN Sezione di Catania, Dipartimento di Fisica, Universitá di Catania, Via Santa Sofia 64, I-95123 Catania, Italy
[2] Dip. di Fisica e Scienze della Terra dell'Università di Ferrara and INFN Sez. di Ferrara, Via Saragat 1, I-44100 Ferrara, Italy
Received 2018 March 29; revised 2018 May 9; accepted 2018 May 18; published 2018 June 21

Abstract

The detection of GW170817 and its electromagnetic counterparts allows us to constrain the equation of state of dense matter in new and complementary ways. Very stiff equations of state are ruled out by the upper limit on the average tidal deformability, $\tilde{\Lambda} \lesssim 800$, imposed by the detected gravitational wave signal. A lower limit, $\tilde{\Lambda} \gtrsim 400$, can also be extracted by considering the large amount of ejected matter that powers the kilonova AT2017gfo. By using several microscopic nucleonic equations of state, we first confirm the existence of a monotonic relation between $R_{1.5}$ (the radius of the $1.5\,M_\odot$ configuration) and $\tilde{\Lambda}$. This translates the limits on $\tilde{\Lambda}$ into limits on the radius: $11.8\,\mathrm{km} \lesssim R_{1.5} \lesssim 13.1\,\mathrm{km}$. We then show that the monotonic relation is violated if a second branch of compact stars composed of quark matter exists, as in the two-families or twin-stars scenarios. In particular, it is possible to fulfill the limits on $\tilde{\Lambda}$ while having $R_{1.5}$ significantly smaller than 12 km. In both of these scenarios, the event GW170817/AT2017gfo originates from the merger of a hadronic star and a star containing quark matter.

Key words: equation of state – gravitational waves – stars: neutron

1. Introduction

The detection of the first signal of gravitational waves (GWs) from the merger of two neutron stars (NSs) in 2017 August, GW170817 (Abbott et al. 2017a), has clearly shown the power of this new observational tool to study the properties of dense matter and its equation of state (EOS). Indeed, it was possible to set the first upper limit on the dimensionless tidal deformability $\Lambda_{1.4}$ of an NS with a mass of $1.4\,M_\odot$:$\Lambda_{1.4} < 800$ at 90% confidence level (for the case of low-spin priors). As a general rule, stiff EOSs lead to NSs with large radii that are easily deformed by the tidal field of the companion and have, correspondingly, a large value of Λ. In Abbott et al. (2017a), it has been shown that some very stiff EOSs such as MS1 and MS1b (Mueller & Serot 1996) are basically ruled out. A number of analyses have confirmed this conclusion: Annala et al. (2018), by using a general polytropic parameterization of the EOS that is compatible with perturbative QCD at a very high density, have shown that $\Lambda_{1.4} < 800$ implies that the radius of a $1.4\,M_\odot$ compact star is $R_{1.4} < 13.4$ km. Similar results have been obtained by Most et al. (2018) and Lim & Holt (2018), where an EOS based on chiral effective field theory has been used up to densities close to nuclear matter saturation density. Raithel et al. (2018) also confirm these findings.

The source of GW170817 has also released two strong electromagnetic signals: a short gamma-ray burst GRB170817A delayed by ∼2 s with respect to the GW signal and a kilonova, AT2017gfo, with a peak of luminosity occurring a few days after the merger (Abbott et al. 2017b, 2017c). The short gamma-ray burst did not show any prolonged activity after the prompt emission: the merger's remnant is therefore most likely a hypermassive star that, in less than one second, has collapsed to a black hole (Margalit & Metzger 2017; Rezzolla et al. 2018; Ruiz et al. 2018).

On the other hand, one can infer that also extremely soft EOSs are ruled out. A first argument is again based on the observation of the short gamma-ray burst: the post-merger remnant did not collapse promptly to a black hole but survived as a hypermassive star for at least a few ms. In turn, this implies that the total mass of the binary system was below the threshold mass for prompt collapse $M_{\rm th}$.[3] The value of $M_{\rm th}$ depends quite strongly on the adopted EOS: the softer the EOS, the lower the value of $M_{\rm th}$. Bauswein et al. (2017) found that GW170817 allows one to set a lower limit on the radius of the $1.6\,M_\odot$ compact star: $R_{1.6} > 10.7$ km, thus excluding very soft EOSs.

Also, the observed kilonova signal provides constraints on the EOS. The kilonova (Alexander et al. 2017; Coulter et al. 2017; Cowperthwaite et al. 2017; Nicholl et al. 2017; Pian et al. 2017) is generated by the mass ejected from the merger. Radice et al. (2018) inferred that the large amount of ejected matter, needed to explain the features of AT2017gfo, implies a not too soft EOS. In particular, the average tidal deformability of the binary,

$$\tilde{\Lambda} = \frac{16}{13}\frac{(M_1 + 12\,M_2)\,M_1^4}{(M_1+M_2)^5}\Lambda_1 + (1 \leftrightarrow 2), \qquad (1)$$

where M_1 and M_2 are the masses of the components, must be larger than about 400. By using the results of Annala et al. (2018), one obtains that $R_{1.4} \gtrsim 12$ km.

Another way to impose limits on the smallest possible value of $R_{1.4}$ is based on incorporating all lab information about the EOS at densities up to saturation. For instance, the PREX collaboration obtained a measurement of the neutron skin of ^{208}Pb (Abrahamyan et al. 2012), and from this measurement, Fattoyev et al. (2018) derived constraints on the density dependence of the symmetry energy, which, in turn, translate into limits on the values of the radius and of the tidal deformability. They obtain $R_{1.4} > 12.55$ km and $\Lambda_{1.4} > 490$. Somehow similarly, the very recent analyses of Most et al. (2018) and Lim & Holt (2018) confirm a lower limit for $R_{1.4} \gtrsim 11.65$–12 km by using state-of-the-art EOSs at sub-nuclear densities. Note that all of these limits are obtained by

[3] Within the two-families scenario (Drago et al. 2014a, 2016; Drago & Pagliara 2016; Wiktorowicz et al. 2017), this implies that the event of 2017 August was not the merger of two NSs, but the merger of a hadronic star and of a strange quark star (Drago & Pagliara 2018).

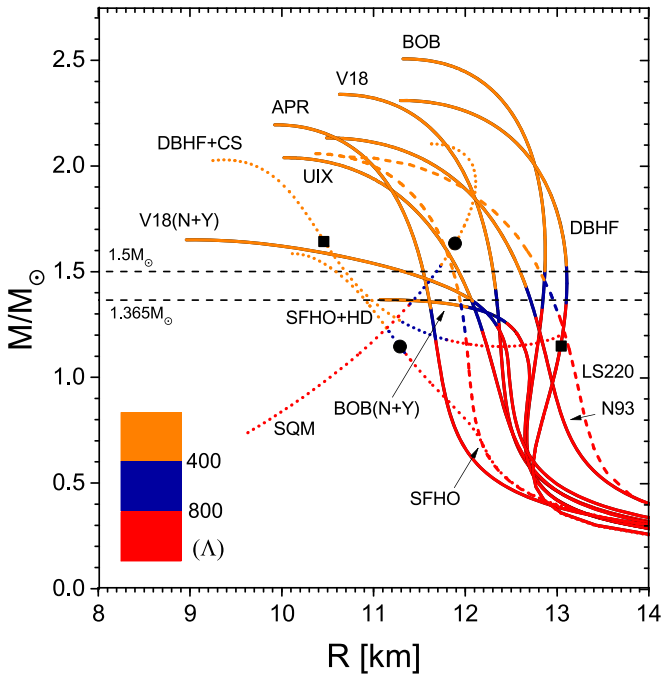

Figure 1. Mass–radius relations for different EOS, indicating also values of the tidal deformability Λ. Solid (dashed) curves show microscopic (phenomenological) EOSs, see the text. Markers indicate the $q = 0.7$ configurations for the two-families (●) and twin-stars (■) scenarios.

assuming that only one family of compact stars exists and that no first-order phase transition to quark matter occurs at large densities.

A more "traditional" technique to constrain the radii of compact stars relies on the modeling of the X-ray spectra of compact stars in LMXBs. Some analyses indicate very small radii: for stars of 1.4–1.5 $M_\odot$, the review paper of Özel & Freire (2016) suggests radii in the range 9.9–11.2 km. Those results have been criticized in Steiner et al. (2010) and Lattimer & Steiner (2014): in particular, if the atmosphere contains He, significantly larger radii are extracted (Lattimer & Steiner 2014). More recently, Steiner et al. (2018) have shown that when allowing for the occurrence of a first-order phase transition in dense matter (Model C), $R_{1.4}$ is smaller than 12 km to 95% confidence, confirming a previous analysis of Steiner et al. (2010). However, $R_{1.4}$ could be larger if NSs have uneven temperature distributions. Clearly, no firm conclusions have yet been reached, and we need to wait for new data, such as that collected by the NICER mission.

In this paper, we investigate under which conditions $R_{1.5} < 12$ km can be consistent with the limits on $\tilde{\Lambda}$ extracted from GW170817/AT2017gfo. As suggested also by Fattoyev et al. (2018), the tension between small radii and not too small $\tilde{\Lambda}$ can be relieved if a strong phase transition occurs at supranuclear densities.

We first present results for the mass–radius relations and tidal deformabilities of NSs as obtained by microscopic calculations of the EOS. We show that $R_{1.5}$ is typically larger than about 11.8 km for $\tilde{\Lambda} \gtrsim 400$ (if the maximum mass is larger than about 2 $M_\odot$). We then explore two possibilities for the appearance of quark matter in compact stars: a first scenario based on the coexistence of two families of compact stars, i.e., hadronic stars (HSs) and quark stars (QSs) (Drago et al. 2014a, 2016; Drago & Pagliara 2016; Wiktorowicz et al. 2017), and a second scenario based on the so called "twin-stars" solution of the Tolman–Oppenheimer–Volkoff (TOV) equation, obtained in the presence of a strong first-order phase transition to quark matter (Schertler et al. 2000; Alford et al. 2015; Paschalidis et al. 2018). We discuss how the formation of quark matter allows us to fulfill the constraints on $\tilde{\Lambda}$ and to obtain at the same time stellar configurations with radii significantly smaller than 11.5 km in the two scenarios discussed above.

2. Equations of State of Dense Matter

Let us first discuss the standard one-family scenario and the modeling of the EOS. At variance with recent calculations using only polytropic EOSs or only phenomenological EOSs with parameters fitted to properties of nuclear matter and finite nuclei around saturation density, we also use here the more reliable "microscopic" EOSs based on many-body calculations. In particular, we examine several EOSs (Li & Schulze 2008) obtained within the Brueckner–Hartree–Fock (BHF) approach to nuclear matter (Jeukenne et al. 1976; Baldo 1999; Baldo & Burgio 2012), which is based on different nucleon–nucleon potentials, i.e., the Argonne V_{18} (V18, UIX) (Wiringa et al. 1995), the Bonn B (BOB) (Machleidt et al. 1987), and the Nijmegen 93 (N93) (Nagels et al. 1978; Stoks et al. 1994) and compatible three-nucleon forces (Grangé et al. 1989; Baldo et al. 1997; Zuo et al. 2002; Li et al. 2008) as input. Furthermore, we compare these with the often-used results of the variational calculation (APR) (Akmal et al. 1998) and the Dirac–BHF method (DBHF) (Brockmann & Machleidt 1990; Li et al. 1992; Gross-Boelting et al. 1999), employing V18 and Bonn A potentials, respectively. Two phenomenological relativistic-mean-field EOS are used for comparison: LS220 (Lattimer & Swesty 1991) and SFHo (Steiner et al. 2013).

Apart from these purely nucleonic EOSs, we also examine EOSs containing hyperons, BOB(NN+NY) (Chen et al. 2011; Schulze & Rijken 2011) and V18(NN+NY+YY) (Rijken & Schulze 2016). Finally, the SFHo with the inclusion of delta resonances and hyperons (SFHO+HD) is also analyzed (Drago et al. 2014b). In particular, we consider two parameterizations corresponding to two different values for the coupling of the delta resonances with the sigma meson: $x_{\sigma\Delta} = 1.15$ (SFHO+HD) and $x_{\sigma\Delta} = 1$ (SFHO+HD2), while we set the couplings with the omega and the rho meson to $x_{\omega\Delta} = x_{\rho\Delta} = 1$. These two choices are motivated by several analyses of scattering data (electron and pion scattering off nuclei), suggesting a coupling with the sigma meson stronger than the coupling with the omega meson (see the discussion in Drago et al. 2014b).

Concerning the quark-matter EOS, we adopt two models representative for the two-families and twin-stars scenario, respectively:

A simple parameterization of a strange-quark-matter EOS encoding both the non-perturbative phenomenon of confinement and the perturbative quark interactions (Weissenborn et al. 2011). We consider two parameters sets: the set QS with $B_{\rm eff}^{1/4} = 137.5$ MeV and $a_4 = 0.7$ whose corresponding maximum mass is $M_{\rm TOV} = 2.1\,M_\odot$, and the set QS2 with $B_{\rm eff}^{1/4} = 142$ MeV and $a_4 = 0.9$ whose corresponding maximum mass is $M_{\rm TOV} = 2.0\,M_\odot$. For the two-families scenario, these EOSs are combined with the hadronic SFHO+HD and SFHO+HD2 EOSs for the low-mass, small-radius partner.

A constant-speed-of-sound EOS (DBHF+CS) to model hybrid stars: one adopts a nucleonic EOS up to a transition pressure $p_{\rm trans}$ and implements a first-order phase transition, which is characterized by an energy density jump Δe at the onset of the phase transition and by the speed of sound of pure quark matter c_q^2. For this study, we have taken the results of (Alford et al. 2015) for the DBHF nucleonic EOS, and we have set $p_{\rm trans}/e_{\rm trans} = 0.1$, $\Delta e/e_{\rm trans} = 1$ and $c_q^2 = 1$. One needs to choose a speed of sound saturating the causal limit, because with more "normal" values, it is impossible to obtain $M_{\rm TOV} \geqslant 2\,M_\odot$ and $R_{1.4} \leqslant 12$ km. Still, a strong fine-tuning of the parameters is needed in order to satisfy all constraints. For comparison, we also consider the parameter set DBHF+CS2: $p_{\rm trans}/e_{\rm trans} = 0.095$, $\Delta e/e_{\rm trans} = 0.65$ and $c_q^2 = 2/3$, which leads to a larger value of $R_{1.4}$.

3. Results and Discussion

For each EOS, we construct the family of solutions of the TOV system with the addition of the equation for the tidal Love number k_2 (Hinderer et al. 2010; Postnikov et al. 2010), which is related to the dimensionless tidal deformability by $\Lambda \equiv (2/3)(R/M)^5 k_2$.

In Figure 1, we display the mass–radius relations for the EOSs adopted here, and we also encode the information on the tidal deformabilities. Note, most importantly, that EOSs that reach the two-solar-mass lower limit and fulfill the constraint $400 < \Lambda_{1.365} < 800$, predict $12\,{\rm km} \lesssim R_{1.5} \lesssim 13\,{\rm km}$, in agreement with the analysis of Annala et al. (2018).

Note also that not all of the EOSs satisfy the two-solar-mass limit: some EOSs in which hyperons and/or delta resonances are also included (in particular SFHO-HD) lead to small maximum masses ($M_{\rm TOV} \approx 1.6\,M_\odot$) and, at the same time, to very compact configurations, $R_{1.5} < 11$ km. Such EOSs would be excluded within the standard one-family scenario in which all compact stars belong to the same family. In that scenario, there is a one-to-one correspondence between the mass–radius relation and the EOS. However, they are allowed if one adopts the so called two-families scenario in which the heaviest stars are interpreted as QSs, whereas the lighter and smaller stars are interpreted as HSs (Drago et al. 2014a, 2016; Drago & Pagliara 2016; Wiktorowicz et al. 2017).

To constrain the EOSs by using the data of the event GW170817, we fix the chirp mass $M_c \equiv (M_1 M_2)^{3/5}/(M_1 + M_2)^{1/5} = 1.188\,M_\odot$ (corresponding to $M_1 = M_2 = 1.365\,M_\odot$ for a symmetric binary system), and compute $\tilde{\Lambda}$, Equation (1), as a function of the mass asymmetry $q = M_2/M_1$. The range deduced for GW170817 was $q = 0.7$–1 (Abbott et al. 2017a), corresponding to a maximum asymmetry $(M_1, M_2) = (1.64, 1.15)\,M_\odot$. The results are displayed in Figure 2. The one-family EOSs predict an effective deformability nearly independent of the asymmetry q. When calculating $\tilde{\Lambda}$ within the two-families scenario, we assume that the binary system is a mixed system with a light HS and a heavy QS, i.e., M_1 refers to a QS (see footnote 3). Similarly, within the twin-stars scenario, we assume that the most massive star is the hybrid star, as in Paschalidis et al. (2018). The configurations corresponding to maximum asymmetry $q = 0.7$ are indicated by markers in Figure 1 for both scenarios. In particular, the twin-stars configuration features a very large difference between the radii of the two components: $(R_1, R_2) = (10.7, 13.0)$ km, which allows one to achieve concurrently a very small radius R_1 and a sufficiently large $\tilde{\Lambda} \approx 600$. Notice that in both of these scenarios, a nonnegligible dependence of $\tilde{\Lambda}$ on q is found.

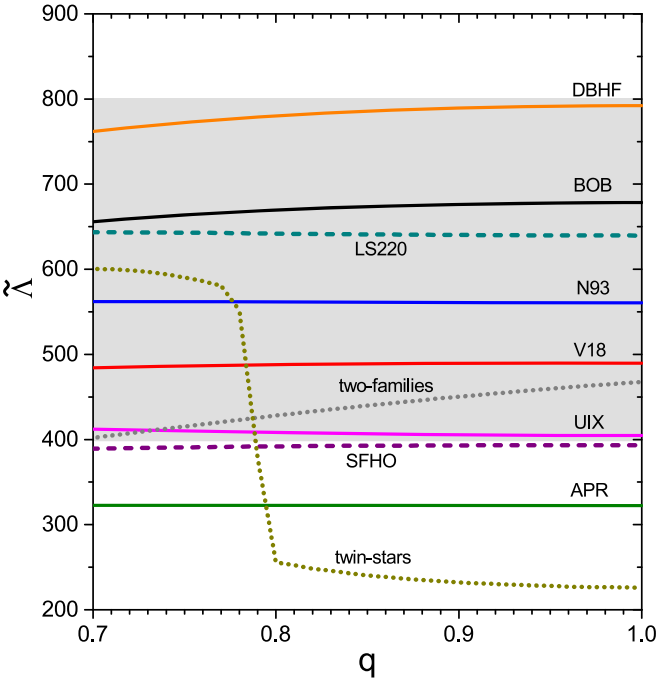

Figure 2. Effective deformability $\tilde{\Lambda}$, Equation (1), vs. mass asymmetry $q = M_2/M_1$ for a binary NS system with fixed chirp mass $M_c = 1.188\,M_\odot$ for different EOSs. The shaded area is constrained by the interpretation of the GW170817 event.

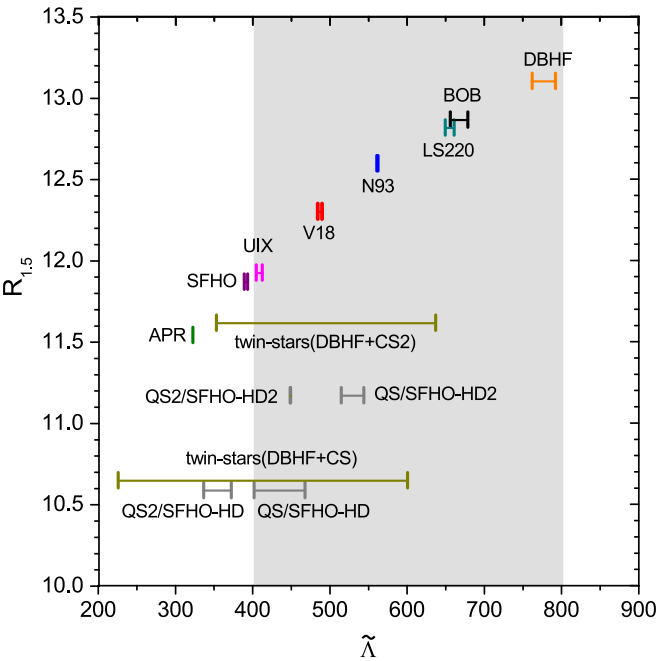

Figure 3. Smallest $R_{1.5}$ radius of an asymmetric binary NS system and possible range of $\tilde{\Lambda}$ with fixed chirp mass $M_c = 1.188\,M_\odot$ and varying $q = 0.7$–1 for different EOSs. For the two-families scenario, we show the results obtained when combining SFHO-HD or SFHO-HD2 with QS or QS2 (in the case QS2/SFHO-HD2 there is no visible dependence on q).

Figure 3 summarizes the main outcome of this study: we display for the different EOSs the correlation between the values of $\tilde{\Lambda}$ (for a fixed $M_c = 1.188\,M_\odot$ and with q varying in

the range 0.7–1) and $R_{1.5}$. In the case of the two-families or twin-stars scenarios, $R_{1.5}$ indicates the radius of the most compact component. Within the one-family scenario, one observes a very tight and monotonic correlation between $R_{1.5}$ and $\tilde{\Lambda}$. All of the EOSs that fulfill the constraint $\tilde{\Lambda} > 400$ from Radice et al. (2018) lead to $R_{1.5} > 11.8$ km. This feature is violated if a second branch of compact stars exists, as in the case of the two families or of the twin stars. Moreover, for some choice of the parameters, it is possible to satisfy $\tilde{\Lambda} > 400$ and obtain stellar configurations with $R_{1.5}$ significantly smaller than 12 km.

Within the twin-stars scenario, an extremely detailed parametric analysis was already performed in Alford et al. (2015) by using the nucleonic EOSs DBHF and BHF (Taranto et al. 2013). There, it was stressed that to obtain $R_{1.5}$ smaller than 12 km, c_q^2 must be significantly larger than one-third. In Figure 3, we have implemented an example (DBHF+CS2) for which $R_{1.5} = 11.6$ km, obtained by fixing $c_q^2 = 2/3$. To reach smaller values of $R_{1.5}$, even larger sound speeds should be assumed. In the causal limit, $c_q^2 = 1$, one obtains $R_{1.5} = 10.7$ km. We have considered here only the nucleonic EOS DBHF because BHF is a rather soft EOS, and it would not be possible to satisfy the limit $\tilde{\Lambda} > 400$. In conclusion, the twin-stars scenario allows one to reach radii smaller than 12 km while satisfying the limit on $\tilde{\Lambda}$, only for a very small parameter space.

Conversely, for the two-families scenario, the parameter space is larger. We can fulfill the limit $\tilde{\Lambda} > 400$ with both the hadronic EOSs SFHO+HD and SFHO+HD2, which lead to $R_{1.5} = 10.6$ km and to $R_{1.5} = 11.2$ km, respectively. Only when combining the soft hadronic EOS SFHO+HD with the soft quark EOS QS2, the limit on $\tilde{\Lambda}$ is not satisfied. Notice that in both quark EOSs $c_q^2 \sim 1/3$.

Let us now compare the two-families and twin-stars scenarios. In the two families, the low-mass objects are made of hadrons and the presence of delta resonances and/or hyperons allows one to reach small radii (and very small values of Λ) for masses in the range (1.4–1.5) $M_\odot$. The more massive stars are instead QSs and their radii are not extremely small (their Λ has an intermediate value). In the twin-stars scenario, the low-mass objects are made of nucleons and have large radii and large Λ, while the most massive stars are hybrid stars with a very large quark content and small radii and Λ. Note how in both these scenarios the event of 2017 August needs to be interpreted as a "mixed case", in which one of the objects is made only of hadrons and the other contains deconfined quarks. While these two scenarios are both able to interpret the event of 2017 August and to have very small values for $R_{1.5}$, the differences in their mass–radius relation and composition will provide different and testable outcomes for the three cases of mergers they are able to produce: HS-HS, HS-QS, and QS-QS in the case of the two-families and NS-NS, NS-hybrid star, and hybrid star-hybrid star in the case of the twin-stars (see Drago et al. 2018 and work in preparation). For instance, in the case of a merger of two light compact stars, e.g., $1.2\,M_\odot + 1.2\,M_\odot$, the twin-stars scenario predicts very large values of $\tilde{\Lambda}$, while for the two-families scenario, $\tilde{\Lambda}$ is significantly smaller. This difference can easily be tested both through the GW signal and through the kilonova.

An open issue regarding both the two-families and the twin-stars scenarios concerns the estimates of the mass ejected during/after the merger and its correlation with $\tilde{\Lambda}$, in the case of a mixed system, HS-QS or NS-hybrid star. Presently, no numerical simulation has been performed for these two scenarios. In particular, within the two-families scenario, the numerical task is very challenging because one has to deal with two different EOSs. However, in both cases, GW170817 can be interpreted as due to the merger of quite an asymmetric system, $q \lesssim 0.8$, in which the low-mass component has a value of Λ exceeding 400. Asymmetric systems lead in general to a larger amount of ejected matter with respect to symmetric systems (Bauswein et al. 2013). Moreover, because the low-mass companion is an HS with a not too small Λ, we expect that most of the ejected mass is provided by the tidal disruption of the HS and that the accretion torus that forms around the post-merger remnant is made of hadronic matter. It will be interesting, in future calculations, to investigate whether the event AT2017gfo can be explained through the material ejected from the HS component of the mixed system in the two-families scenario.

4. Conclusions

While the standard interpretation of the GW170817 event in the one-family scenario is perfectly compatible with the merging of two nucleonic NSs governed by a microscopic nuclear EOS respecting the $M_{\rm TOV} > 2\,M_\odot$ limit, we have shown here that the lower limit on the tidal deformability obtained by Radice et al. (2018) is not incompatible with $R_{1.5}$ being even significantly smaller than 12 km if one assumes that the population of compact stars is not made of only one family. Indeed, when allowing for the existence of disconnected branches in the mass–radius relation, either within the two-families scenario or within the twin-stars scenario, one can explain the existence of very compact stars and at the same time one can fulfill the request of having a not too small average tidal deformability, as suggested by the analysis of AT2017gfo.

Notice that in both scenarios, the source of GW170817 is a mixed binary system: a HS and a QS within the two-families scenario (Drago & Pagliara 2018) and a hybrid star and a nucleonic star within the twin-stars scenario (Paschalidis et al. 2018). It is interesting to note that within the two-families scenario, a system with the chirp mass of the source of GW170817 cannot be composed of two HSs: such a system would have too small an average tidal deformability, and moreover it would lead to a prompt collapse (Drago & Pagliara 2018). In this respect, the constraint on the tidal deformability and the evidence of formation of a hypermassive star within the event GW170817 both suggest that one of the two stars must be a QS, if the hypothesis of the two families of compact stars is adopted.

Most of the analyses suggesting limits on the radii are based on a statistical average of a few stellar objects. It is therefore possible that some of those objects have radii even significantly larger than the average. A feature of the two-families scenario concerns the mass distribution of HSs and QSs. There exists a "coexistence mass range" in which compact stars can be both HSs or QSs. In Wiktorowicz et al. (2017), a population-synthesis analysis has shown that the fraction of QSs in LMXBs in that mass range is not marginal, up to 30% or more. It is therefore possible that some of the "NSs" in an LMXB are actually QSs and have a radius of about (11.5–12) km. The analysis of the X-ray signal emitted by a QS in an LMXB is, though, still a rather unexplored problem (Zdunik et al. 2001;

Kovacs et al. 2009), and at the moment it is very difficult to indicate how to distinguish a QS from an NS solely from the properties of its X-ray spectrum. It is interesting to remark that Nättilä et al. (2017) suggest for the NS in 4U 1702429 a radius of 12.4 ± 0.4 km for a mass of $1.9 \pm 0.3\, M_{\odot}$, which nicely sits on our QS branch.

Future measurements of GWs from binary collisions could provide us with even tighter constraints on the tidal deformability by accumulating data from several GW events (Agathos et al. 2015). Moreover, very soon, the NICER collaboration will release results for the measurements of the radii of the closest pulsars. Therefore, in the near future, we expect to have a crucial opportunity to test the hypothesis that quark matter does form in compact stars. Finally, another complementary way to study the properties of dense matter relies on the measurement of the moment of inertia: the future SKA experiment will face this task. In a forthcoming paper, we will present our predictions for the moment of inertia of compact stars in the standard one-family scenario and in the two-families scenario.

References

Abbott, B., Abbott, R., Abbott, T. D., et al. 2017a, PhRvL, 119, 161101
Abbott, B. P., Abbott, R., Abbott, T. D., et al. 2017b, ApJL, 848, L13
Abbott, B. P., Abbott, R., Abbott, T. D., et al. 2017c, ApJL, 848, L12
Abrahamyan, S., Ahmed, Z., Albataineh, H., et al. 2012, PhRvL, 108, 112502
Agathos, M., Meidam, J., Del Pozzo, W., et al. 2015, PhRvD, 92, 023012
Akmal, A., Pandharipande, V. R., & Ravenhall, D. G. 1998, PhRvC, 58, 1804
Alexander, K. D., Berger, E., Fong, W., et al. 2017, ApJL, 848, L21
Alford, M. G., Burgio, G. F., Han, S., Taranto, G., & Zappalà, D. 2015, PhRvD, 92, 083002
Annala, E., Gorda, T., Kurkela, A., & Vuorinen, A. 2018, PhRvL, 120, 172703
Baldo, M. 1999, in Nuclear Methods and the Nuclear Equation of State, ed. M. Baldo (Singapore: World Scientific), 1
Baldo, M., Bombaci, I., & Burgio, G. F. 1997, A&A, 328, 274
Baldo, M., & Burgio, G. F. 2012, RPPh, 75, 026301
Bauswein, A., Goriely, S., & Janka, H. T. 2013, ApJ, 773, 78
Bauswein, A., Just, O., Janka, H.-T., & Stergioulas, N. 2017, ApJL, 850, L34
Brockmann, R., & Machleidt, R. 1990, PhRvC, 42, 1965
Chen, H., Baldo, M., Burgio, G. F., & Schulze, H.-J. 2011, PhRvD, 84, 105023
Coulter, D. A., Foley, R. J., Kilpatrick, C. D., et al. 2017, Sci, 358, 1556
Cowperthwaite, P. S., Berger, E., Villar, V. A., et al. 2017, ApJL, 848, L17
Drago, A., Lavagno, A., & Pagliara, G. 2014a, PhRvD, 89, 043014
Drago, A., Lavagno, A., Pagliara, G., & Pigato, D. 2014b, PhRvC, 90, 065809
Drago, A., Lavagno, A., Pagliara, G., & Pigato, D. 2016, EPJA, 52, 40
Drago, A., & Pagliara, G. 2016, EPJA, 52, 41
Drago, A., & Pagliara, G. 2018, ApJL, 852, L32
Drago, A., Pagliara, G., Popov, S. B., Traversi, S., & Wiktorowicz, G. 2018, Univ, 4, 50
Fattoyev, F. J., Piekarewicz, J., & Horowitz, C. J. 2018, PhRvL, 120, 172702
Grangé, P., Lejeune, A., Martzolff, M., & Mathiot, J.-F. 1989, PhRvC, 40, 1040
Gross-Boelting, T., Fuchs, C., & Faessler, A. 1999, NuPhA, 648, 105
Hinderer, T., Lackey, B. D., Lang, R. N., & Read, J. S. 2010, PhRvD, 81, 123016
Jeukenne, J. P., Lejeune, A., & Mahaux, C. 1976, PhR, 25, 83
Kovacs, Z., Cheng, K. S., & Harko, T. 2009, A&A, 500, 621
Lattimer, J. M., & Steiner, A. W. 2014, ApJ, 784, 123
Lattimer, J. M., & Swesty, F. D. 1991, NuPhA, 535, 331
Li, G. Q., Machleidt, R., & Brockmann, R. 1992, PhRvC, 45, 2782
Li, Z. H., Lombardo, U., Schulze, H.-J., & Zuo, W. 2008, PhRvC, 77, 034316
Li, Z. H., & Schulze, H.-J. 2008, PhRvC, 78, 028801
Lim, Y., & Holt, J. W. 2018, arXiv:1803.02803
Machleidt, R., Holinde, K., & Elster, C. 1987, PhR, 149, 1
Margalit, B., & Metzger, B. D. 2017, ApJL, 850, L19
Most, E. R., Weih, L. R., Rezzolla, L., & Schaffner-Bielich, J. 2018, arXiv:1803.00549
Mueller, H., & Serot, B. D. 1996, NuPhA, 606, 508
Nagels, M. M., Rijken, T. A., & de Swart, J. J. 1978, PhRvD, 17, 768
Nättilä, J., Miller, M. C., Steiner, A. W., et al. 2017, A&A, 608, A31
Nicholl, M., Berger, E., Kasen, D., et al. 2017, ApJL, 848, L18
Özel, F., & Freire, P. 2016, ARA&A, 54, 401
Paschalidis, V., Yagi, K., Alvarez-Castillo, D., Blaschke, D. B., & Sedrakian, A. 2018, PhRvD, 97, 084038
Pian, E., D'Avanzo, P., Benetti, S., et al. 2017, Natur, 551, 67
Postnikov, S., Prakash, M., & Lattimer, J. M. 2010, PhRvD, 82, 024016
Radice, D., Perego, A., Zappa, F., & Bernuzzi, S. 2018, ApJL, 852, L29
Raithel, C., Özel, F., & Psaltis, D. 2018, ApJL, 857, L23
Rezzolla, L., Most, E. R., & Weih, L. R. 2018, ApJL, 852, L25
Rijken, T. A., & Schulze, H.-J. 2016, EPJA, 52, 21
Ruiz, M., Shapiro, S. L., & Tsokaros, A. 2018, PhRvD, 97, 021501
Schertler, K., Greiner, C., Schaffner-Bielich, J., & Thoma, M. H. 2000, NuPhA, 677, 463
Schulze, H.-J., & Rijken, T. 2011, PhRvC, 84, 035801
Steiner, A. W., Heinke, C. O., Bogdanov, S., et al. 2018, MNRAS, 476, 421
Steiner, A. W., Hempel, M., & Fischer, T. 2013, ApJ, 774, 17
Steiner, A. W., Lattimer, J. M., & Brown, E. F. 2010, ApJ, 722, 33
Stoks, V. G. J., Klomp, R. A. M., Terheggen, C. P. F., & de Swart, J. J. 1994, PhRvC, 49, 2950
Taranto, G., Baldo, M., & Burgio, G. F. 2013, PhRvC, 87, 045803
Weissenborn, S., Sagert, I., Pagliara, G., Hempel, M., & Schaffner-Bielich, J. 2011, ApJL, 740, L14
Wiktorowicz, G., Drago, A., Pagliara, G., & Popov, S. B. 2017, ApJ, 846, 163
Wiringa, R. B., Stoks, V. G. J., & Schiavilla, R. 1995, PhRvC, 51, 38
Zdunik, J. L., Haensel, P., & Gourgoulhon, E. 2001, A&A, 372, 535
Zuo, W., Lejeune, A., Lombardo, U., & Mathiot, J. F. 2002, EPJA, 14, 469